LIMNOLOGY
and
OCEANOGRAPHY: METHODS

Limnol. Oceanogr.: Methods 7, 2009, 371–381

Determination of ultra-low oxygen concentrations in oxygen minimum zones by the STOX sensor

Niels Peter Revsbech[1], Lars Hauer Larsen[2], Jens Gundersen[2], Tage Dalsgaard[3], Osvaldo Ulloa[4], and Bo Thamdrup[5]*

[1]Department of Biological Sciences, University of Aarhus, Building 1540, DK-8000 Aarhus C, Denmark

[2]Unisense A/S, Brendstrupgaardsvej 21 F, DK-8200 Aarhus N, Denmark

[3]National Environmental Research Institute, University of Aarhus, Vejlsøvej 25, DK-8600 Silkeborg, Denmark

[4]Department of Oceanography and Center for Oceanographic Research, Universidad de Concepcion, Casilla 160-C, Concepcion, Chile

[5]Nordic Center for Earth Evolution, Institute of Biology, University of Southern Denmark, DK-5230 Odense, Denmark

Abstract

The methods used until now have not been able to reliably resolve O_2 concentrations in oceanic oxygen minimum zones below 1-2 µmol L^{-1}. We present a new amperometric sensor for the determination of ultra-low O_2 concentrations under in situ conditions. The electrochemical STOX O_2 sensor contains a primary sensing cathode and a secondary cathode that, when polarized, prevents entry of O_2 into the sensor. This arrangement enables frequent in situ zero calibration and confers the sensor with a detection limit of 1-10 nmol L^{-1} O_2, even during application on a Conductivity-Temperature-Depth (CTD) profiler at great water depths. The sensor was used during the Galathea 3 Expedition to demonstrate that the core of the oxygen minimum zone (OMZ) off Peru contained < 2 nM O_2. Application in a reactor on board demonstrated that changes in O_2 concentrations in OMZ water containing < 200 nmol L^{-1} O_2 could be monitored over periods of hours to days. The linear decrease in O_2 concentration in the reactor indicated very low (< 20 nmol L^{-1}) half saturation constants for the O_2 respiring microbial community.

Introduction

Oxygen concentration is one of the most frequently measured parameters in oceanography, as well as in other biological or environmental sciences. Winkler titration is the traditional method for determining O_2 content (e.g., Grasshoff 1983), and spectrophotometric modifications have been developed for low O_2 concentrations (Broenkow and Cline 1969; Labasque et al. 2004), but most O_2 determinations are now performed in situ by use of amperometric or voltammetric oxygen sensors or by fluorescence-based optodes (Glazer et al. 2004; Martini et al. 2007). The Winkler methods have limitations when determining very low O_2 concentrations, and there may be interference from other chemical species, such as NO_2^-, in which case special procedures may be necessary (Morrison et al. 1999). Contributing factors to the difficulties encountered with determination of very low in situ O_2 levels by Winkler methods is introduction of O_2 during sampling and addition of reagents. The sensor-based methods do not require contamination-prone sampling and addition of reagents, and the electrical signals resulting from either the reduction of O_2 within the sensors or from the fluorescence of a fluorophore can be read at extremely high resolution. It is thus, in principle, possible to resolve extremely low O_2 concentrations by use of sensors. However, changes in sensor signal for zero oxygen caused by factors such as temperature and pressure changes combined with electronic offsets have until now resulted in detection limits of typically 1–2 µmol L^{-1} for in situ deployments, with the need for calibration with samples analyzed by Winkler methods. Thus, the general experience by oceanographers, irrespective of whether Winkler methods, electrochemical sensors, or optodes are used, is that O_2 concentrations below a couple of µmol L^{-1} cannot be reliably resolved (Morrison et al. 1999; Paulmier and Ruiz-Pino in press).

*Corresponding author: E-mail: Revsbech@biology.au.dk

Acknowledgments

We are grateful for the technical assistance of Preben Sørensen and Frank Knudsen. The high-quality electronics for laboratory use were constructed by Volker Meyer. The master and crew onboard the Danish Naval Vessel "Vædderen" are thanked for their help and hospitality. Financial Support was given by the Danish Natural Science Research Council, the Danish National Research Foundation, the Chilean National Commission for Scientific and Technological Research (CONICYT) through the FONDAP Program, the Agouron Institute, and the Gordon and Betty Moore Foundation. Part of the present work was carried out during the Galathea 3 expedition under the auspices of the Danish Expedition Foundation. This is Galathea 3 contribution no. P26.

As a consequence of the limitations imposed by the available analytical techniques, O_2 levels in oxygen minimum zones (OMZs) and other oxygen-deficient environments have usually been described as less than some detection limit. As an example, Morrison et al. (1999) described water masses at depths from 200 to 800 m along a 1000-km–long transect in the Arabian Sea as having O_2 concentrations of less than 2.2 μmol L^{-1}. Such detection limits are high compared with those of other biogeochemically important seawater constituents such as nutrients (e.g., Holmes et al. 1999; Patey et al. 2008) and redox active compounds (e.g., Luther et al. 2008; Moffett et al. 2007), and this poor resolution limits our understanding of the effect of O_2 on both microbial and abiotic processes. A pertinent example concerns the regulation of denitrification, which in oxygen minimum zones appears to be inhibited by O_2 concentrations at or below the conventional detection limit (Devol 1978; Bange et al. 2005). This sensitivity potentially explains the experimentally observed dominance of anaerobic ammonium oxidation over organotrophic denitrification as a nitrogen sink in OMZs (Kuypers et al. 2005, Jensen et al. 2008), but more reliable O_2 determinations are necessary for the verification of this hypothesis. As a tool for such investigations, we here present a new amperometric oxygen sensor with built-in capability for in situ zero calibration, and its use in the OMZ of the eastern tropical South Pacific.

Materials and procedures

Sensor principle—The STOX (Switchable Trace amount OXygen) sensor that was developed is depicted in Fig. 1. It is basically an oxygen microsensor with guard cathode as the one described by Revsbech (1989); however, this oxygen microsensor is placed within an additional microsensor capillary and behind an additional membrane and gold cathode. The cathode of the outermost oxygen microsensor is made porous, so that O_2 can pass through the gold matrix and into the inner oxygen microsensor when the gold matrix is depolarized. When polarized at about –0.8 V the gold matrix of the outermost cathode (hereafter named the front guard) will reduce the incoming O_2, and no or very little O_2 will reach the inner electrode. This arrangement thus enables in situ zero calibration.

Sensor construction—The sensor was constructed using the same techniques as described by Revsbech and Jørgensen (1986) and Revsbech (1989). To obtain a high signal enabling detection of very low O_2 concentrations, the inner tip diameter of the outer capillary was increased to 50-100 μm. To enable use with standard sensor holders traditionally used for oceanographic applications, the outer casing was constructed from Schott AR glass with an outer diameter (OD) of 8 mm and an inner diameter (ID) of 7 mm. The inner sensors outer casing was Schott AR glass with an OD of 6 mm and an ID of 5 mm. The central cathode of the inner sensor was made from Schott 8512 glass with an OD of 4 mm and an ID of 2.5 mm. The front guard was made from a 0.6-0.8-mm thick glass capillary (made from either Schott 8533 or AR glass). Into the glass capillary was melted a 5-cm piece of tapered (Revsbech and Jørgensen 1986) 0.05 mm platinum wire from which the glass coating was removed from the outermost 200-400 μm by immersion into HF (a drop of 30% HF covered by mineral oil and contained in a plastic spectrophotometer cuvette). The tip of the tapered platinum (diameter 10-20 μm) was subsequently gold plated in 50% saturated $AuCl_3$ under the microscope using first an applied voltage of –0.7 V (versus a platinum wire inserted into the plating solu-

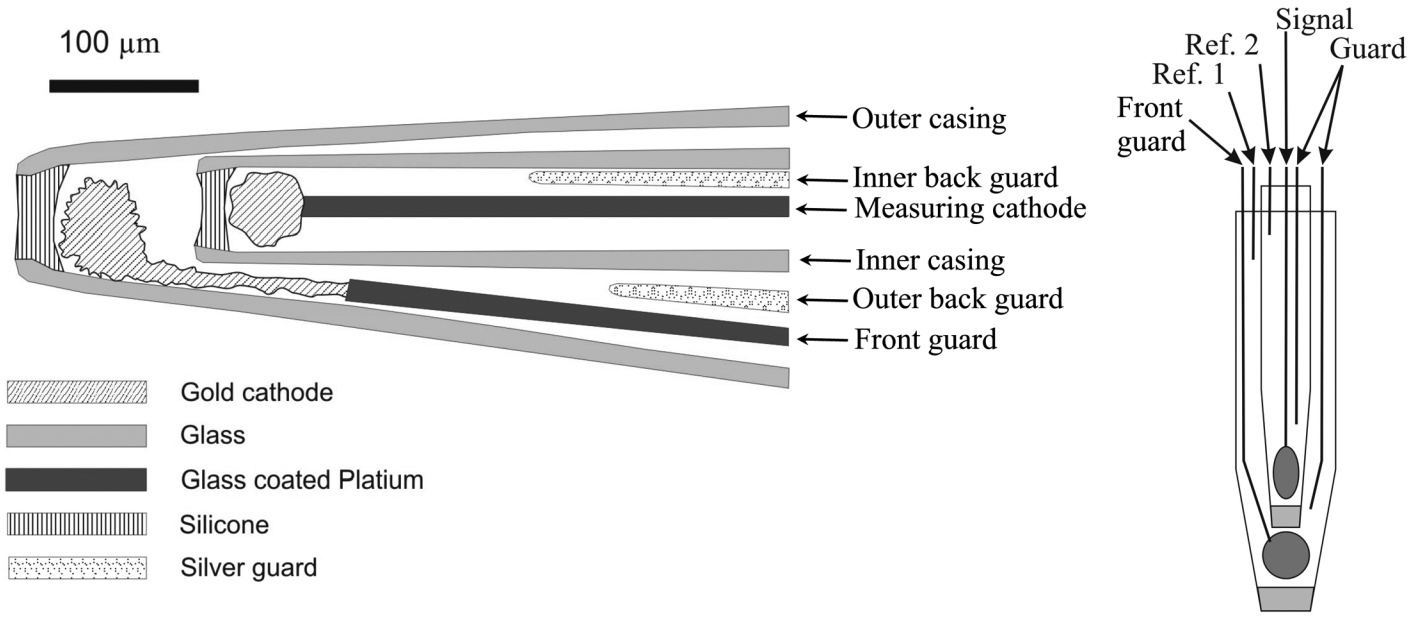

Fig. 1. Left: Schematic drawing of STOX microsensor tip. Not visible are the Ag/AgCl internal references in both inner and outer electrolyte reservoirs. Right: Diagram showing all anodes and cathodes in a STOX sensor.

tion) until the gold ball had a diameter corresponding to about 70% of the inner sensor tip diameter, and finally a voltage of –2.3 V for a fraction of a second. The final plating at –2.3 V resulted in a very porous gold matrix. The gold matrix should, however, not be too porous and soft, as it will then tend to collapse during insertion. The removal of glass from the tip 200-400 µm section of the front guard minimized the risk of glass cracks by insertion of the inner microsensor. The back guard cathodes and the reference anodes inserted into both electrolyte compartments were all made from Teflon-coated silver wire (0.25 mm silver wire with 0.025 mm Teflon coating, World Precision Instruments), from which the Teflon coating was removed from the tip region. The 2-cm tips (insertion ends) of the anodes were electrolytically coated with AgCl as described by Thomas (1978). The silver guards were tapered in KCN solution as also described for platinum by Revsbech and Jørgensen (1986). Electrical contact to the platinum wire of the front guard was made by a similar Teflon-coated silver wire that was pushed into the 1-mm thick capillary. The use of the Teflon-coated silver wire made it possible to avoid any kind of soldering or other fusions of conductors near the sensor, as it is a general experience that soldering near humid glass surfaces may result in erratic currents. It was still necessary to solder gold pins for electrical connections to the silver wire, but these fusions were not in the immediate vicinity of the sensor. One problem by use of Teflon is that it is almost impossible to fasten by gluing, so to create permanent immobilizations we made a knot on the wire that could be covered by UV-curing cement (Loctite 190672, Loctite Corp.) and fixed onto the glass shaft. This cement was also used for all other seals. The silicone membranes were made by inserting the tip of the outer casing into acetic acid-curing silicone rubber (Wacker Elastosil E43, Wacker Chemie) and letting the capillary force draw in silicone. One centimeter long capillaries penetrated the seal of the electrolyte reservoirs to allow injection of mineral oil contained within the sensor holder so that pressure differences across the sensor membrane could be relieved during in situ application. The capillaries were sealed at the top end until mounting on the deep-sea electronics unit and associated sensor holder, when they were opened.

Sensor calibration—For laboratory use, the sensors were calibrated in a glass culture flask (volume 546 mL) with a butyl rubber stopper. The bottle contained 40 mM TRIS (tris[hydroxymethyl]aminomethane) buffer at pH 7.0 that had been purged with nitrogen. The rubber stopper was penetrated by a STOX sensor and a 15-cm long, liquid-filled glass capillary with an inner diameter of 1.5 mm. Care was taken to exclude any gas bubbles within the bottle. A magnetic stirrer kept the solution within the bottle well mixed. The Teflon-coated stirring magnet was melted into a glass tube to avoid leakage of oxygen from the Teflon. About 12 h before the start of the calibration, 1 mL of 1 M sodium ascorbate was injected into the bottle through the rubber stopper to reduce the O_2 concentration. The relatively long half-life of O_2 at the relatively low pH and low ascorbate concentration made it possible to perform a calibration without excessive consumption of O_2 during the procedure. Calibration was performed by injecting small volumes (0.1–0.2 mL) of air-saturated water through the rubber stopper. After each calibration series, 1 mL of 10 M NaOH was injected into the bottle to increase the O_2 consumption rate of the ascorbate so that a reading for practically absolute zero could be obtained. The temperature dependence of the STOX signal was determined by monitoring the change in signal when water that had been air-saturated at 30°C was being cooled down from 30 to 2°C-4°C. The water was contained in a bottle similar to the one used for calibration, and thus, there was no contact with the atmosphere during the experiment. The experiment was repeated with 3 sensors.

During measurement in the OMZ the O_2 readings from one of the two standard oxygen sensors (SBE43) of the Seabird CTD (SBE911) at low but detectable O_2 concentrations were used to calibrate the O_2 response of the STOX microsensor at relevant water depths, temperatures, and oxygen concentrations. The STOX sensors are sufficiently stable long-term to allow calibration before deployment, and the temperature coefficients are almost identical among sensors, but in this first field test, focus was on detection of very low oxygen concentrations and not on the measurement of full O_2 profiles throughout the water column.

Electronics—For laboratory use at sea, we applied a PA2000 picoammeter (Unisense). Polarization and depolarization of the front guard were mediated by inserting a banana jack with connection to the front guard into either the guard or reference socket. For subsequent land-based work, we applied a custom-built picoammeter with timer-controlled switching between front guard on and off. The signal was recorded by either a strip-chart potentiometer recorder or by a Unisense ADC816 16-bit A/D converter. For in situ use, we applied electronics housed into a light-metal alloy cylinder that was designed to resist an external pressure of 600 atm (prototype made by Unisense). In addition to the usual electronics for in situ oxygen microsensor application, the cylinder also housed a timer that could be programmed for continuous shifts between front guard polarization/depolarization with variable intervals. For this study, the timer was set to continuous 20-s front guard on, 40-s off cycles. The timer-controlled switching caused a noise signal that could be used to identify the on-off cycles in anoxic environments where there was otherwise no visible change in sensor signal. The unit supported two STOX sensors attached to the front end. The rear end of the electronics cylinder was equipped with a cable that allowed interfacing with the Seabird CTD. The CTD thus supplied the electronics with power and served to collect the data from the STOX sensor. As the Seabird was equipped with a rather low-resolution 12-bit AD converter (counts 0-4095), we chose to sample only the 0–450 pA region of the STOX sensor output, although the signal from a typical sensor was around 2000 pA for air saturation. The STOX sensors were interfaced with the

electronics cylinder by use of a custom-built Plexiglas sensor holder with oil pressure compensation as described by Reimers and Glud (2000).

The Seabird SBE911 CTD was mounted on a SBE32 rosette water sampler carrying 12 30-L Niskin bottles, and the STOX electronics cylinder was suspended in 4-mm Nylon lines in the center of the rosette. A total of 3 lines were fastened to the top end of the cylinder and an additional 3 to the bottom end. By fastening these lines at an about 45° angle from the vertically held cylinder, the cylinder was positioned in the center of an elastic suspension that protected the rather fragile STOX sensors against mechanical shocks. The CTD was equipped with two sensors each for conductivity (SBE4), temperature (SBE3), and oxygen (SBE43), which were calibrated before and after the Galathea3 Expedition by the manufacturer (C and T) or at the Danish Institute for Fisheries Research (O_2), showing negligible drift.

Experimental area and sampling—We chose to test the new oxygen sensor during the Danish Galathea 3 Expedition during Legs 13 and 14 in February 2007, when the expedition's scientific party sampled the oxygen minimum zone off northern Chile and Peru. Profiles were measured along a track following the coast from 20°03.47′S, 70°45.28′W to 13°52.31′S, 76°47.94′W. The in situ data presented and discussed in this paper were recorded at 14°14.21′S, 76°36.12′W, 36 km off the coast of Southwestern Peru. Data from the shipboard reactor experiment is based on water collected from 60 m depth in the OMZ at 12°26.59′S, 77°35.97′W.

Profiling of the OMZ—When probing with the STOX sensor, the Seabird CTD was positioned at discrete water depths, for about 3 min each, on up-casts. For example, in the up-cast highlighted here, measurements were made at 500, 400, 201, 120, 100, 61, 45, and 31 m depth. Each cycle of STOX front cathode on/off lasted for 1 min, and thus, it was ensured that we had at least 2 complete cycles at each depth.

Reactor experiments—Seawater from 60 m depth in the upper part of the OMZ was investigated in a reactor study to gain insight into the O_2 consumption rates within these water masses at extremely low dissolved O_2. The reactor consisted of a cylindrical glass beaker with an inner diameter of 10 cm and a height of 20 cm. The beaker was closed with a 2-cm thick PVC piston that could slide inside the beaker like a plunger. The space between the PVC and the glass wall was sealed with two butyl rubber O-rings that gave a very tight fit. The reactor could thus be filled without headspace, and by pressing the lid, it was possible to decrease the volume during incubations when withdrawing samples. A 20-mL cut-off glass syringe with a ground glass piston fixed in the lid buffered small change in volume, and thereby, also made it possible to make small amendments without moving the PVC piston. Ports for making amendments and for withdrawing samples were made by fixing 1/8″ and 1/16″ PEEK tubing in holes in the PVC with Upchurch Scientific flangeless fittings, and the STOX-sensor was fitted in an 8-mm hole with a butyl rubber O-ring seal. The reactor had an opening on the side close to the bottom with a ground glass stop cock through which the reactor was filled and bubbles could be removed. When filling the vessel this was attached directly to a Niskin bottle with Iso-Versinic (Saint-Gobain) tubing, and the water was allowed to flow out through the 8-mm hole in the PVC piston. Initially the piston was in the lowest position and the volume below the piston (ca. 100 mL) was filled quickly while all bubbles were removed and water was allowed to overflow for 3 volume changes. The piston was then retracted slowly, still allowing water to flow out through the 8 mm hole. After the piston reached the uppermost position water was allowed to continue to flow for another 3 volume changes. Small volumes of oxygenated seawater were injected at intervals to maintain oxic conditions while keeping the O_2 concentration below 200 nM. During the experiments the reactor was submersed in a water bath maintained at 15.5 ± 0.2°C using an external thermostat. All experiments were conducted within 24 h of sampling. After monitoring the rate of O_2 decrease, 3 mL 7M $ZnCl_2$ was added to the reactor to inhibit microbial respiration to reveal any leakage of O_2 into the reactor.

Assessment

Sensor performance—A typical cycle of front guard depolarization/polarization is shown in Fig. 2 for atmospheric (273 µmol L^{-1}) O_2 saturation and anoxia (0.1 M ascorbate, pH 12) at room temperature (22°C). Notice that the zero signal in ascorbate, when there is no difference between front guard on or off, is significantly lower than the reading with front guard on at atmospheric concentration. From the differences in "front guard on" signals it can be estimated that the front guard for this particular sensor only consumed 98.3% of the incoming O_2. A calibration of a STOX sensor should thus not be based on the difference between a fixed zero and a signal for O_2 as it is done by other amperometric oxygen sensors, but should instead be based on the difference between signal for front guard on and off (Eqs. 1 and 2).

$$\text{Cal. fact.} = \frac{K_{depol} - K_{pol}}{\text{Cal. } O_2 \text{ conc.}} \quad (1)$$

$$O_2 \text{ conc.} = \frac{U_{depol} - U_{pol}}{\text{Cal. fact.}} \quad (2)$$

Here the calibration factor (Cal. fact.) is calculated from the sensor signal (in pA or V output from the picoammeter) in water with known O_2 concentration (Cal. O_2 conc.) with the front guard depolarized (K_{depol}) and polarized (K_{pol}). An unknown O_2 concentration (O_2 conc.) is calculated from the sensor signal with the front guard depolarized (U_{depol}) and polarized (U_{pol}). By doing the calibration this way an efficiency of only 99% or even 90% of the front guard will have very little or no effect on the linearity or detection limit of the sensor. The raw data from a calibration in dilute ascorbate at pH 7 is shown in Fig. 3. Even without addition of any O_2, there

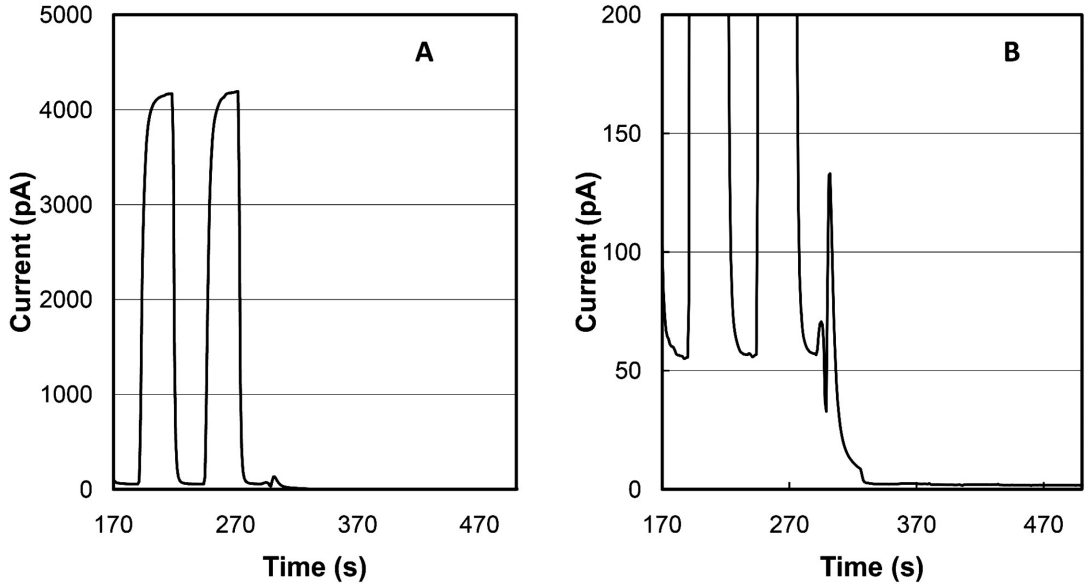

Fig. 2. STOX sensor signal during front cathode on-off cycles while measuring in first air-saturated water and thereafter in anoxic ascorbate solution (A). The signal at low currents is shown in detail (B) to illustrate the—in this case—only 98.7% efficiency of the front cathode removal of O_2.

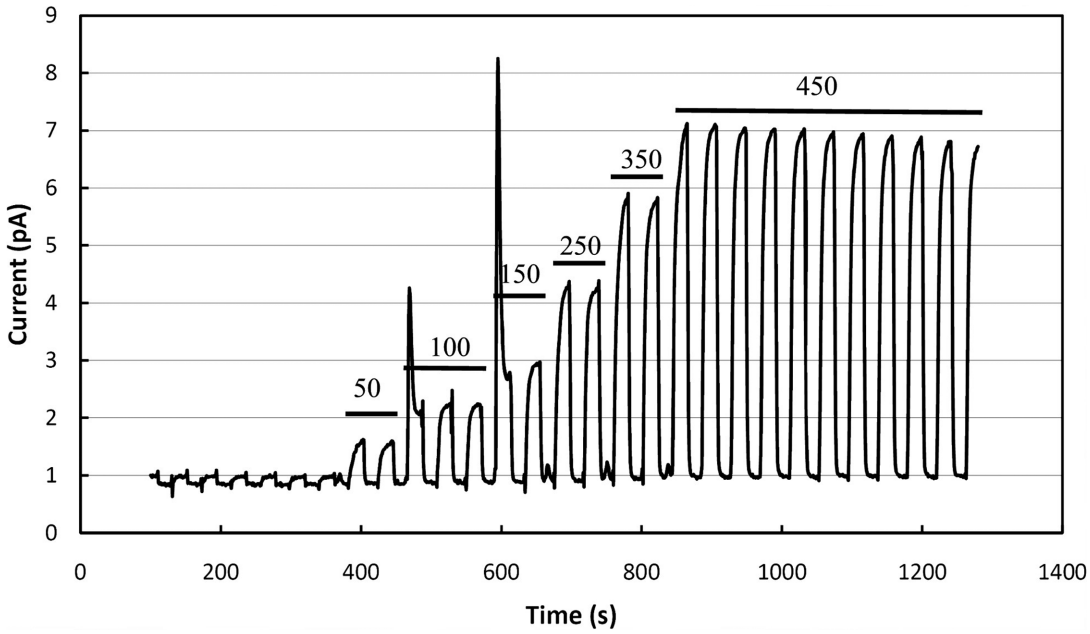

Fig. 3. Sensor signal during calibration of a STOX sensor in a 546-mL bottle. The low signal before addition of small volumes of air-saturated water represents 10 nM O_2. The bars with concentrations (in nM) written above indicate the concentrations that in the absence of any O_2 consumption and the initial 10 nM should have been present during these periods.

was a small signal increase of 0.13 pA when the front guard was depolarized, indicating that some O_2 was present. Subsequent additions of three 0.1 mL aliquots and thereafter two 0.2 mL aliquots resulted in progressively higher signals, and also the signal for front guard on increased a little. The two large "irregular" peaks were due to imperfect mixing of the water within the bottle before front guard depolarization. The signal for a total of 0.9 mL water added would correspond to a concentration of 450 nM O_2. However, due to the presence of ascorbate in the bottle, consumption of O_2 occurred during the experiment and from the rate of decrease after the last 0.2 mL water addition, a half-life for O_2 of 95 min was calculated.

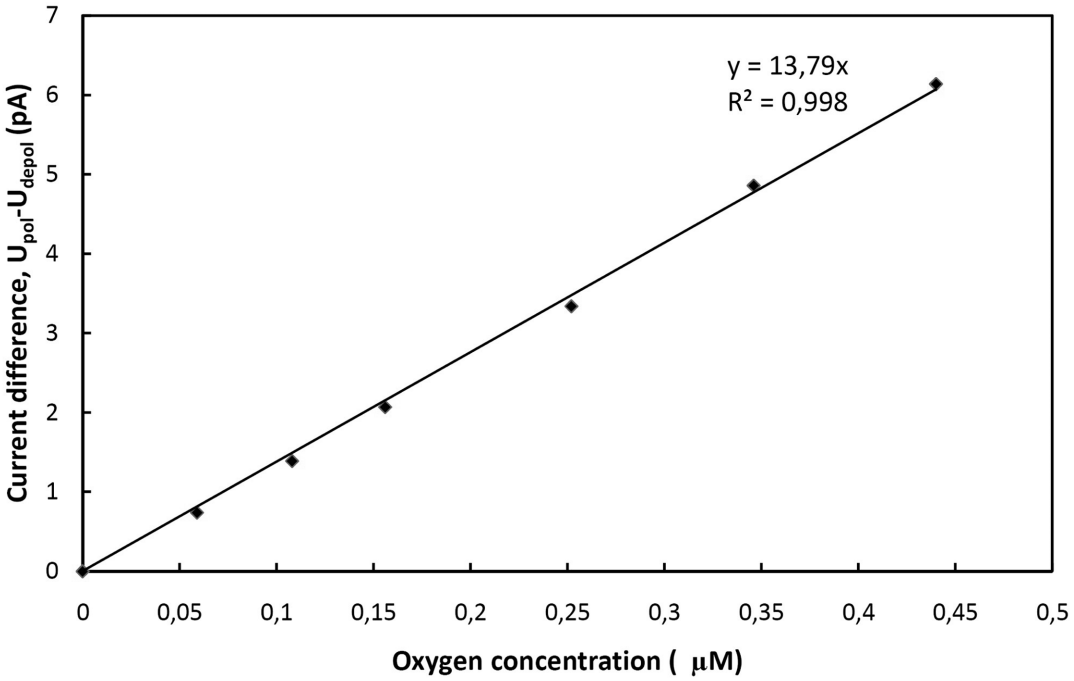

Fig. 4. Calibration curve obtained from the data in Fig. 4. The calibration curve is corrected for an initial concentration of 10 nM and an exponential decay of O_2 in the ascorbate solution. The sensor current shown is the difference between the signals with front guard on and off.

A calibration curve obtained from the data in Fig. 3 is shown in Fig. 4. The calibration curve was calculated from the second polarization/depolarization cycle after each water addition, and the readings were corrected for the consumption between injection and reading assuming a half-life of 95 min. The calculated concentrations were also corrected for the initial signal difference of 0.13 pA that corresponded to 10 nmol L^{-1} O_2. For most sensors, it was possible to resolve a 0.1 pA signal change by front guard on/off, and with a current of 2000-4000 pA for air saturation, this corresponds to a detection limit of about 5-10 nM. In the present example, it would have been possible to detect concentrations down to 1-2 nM. That the initial O_2 concentration of 10 nmol L^{-1} was "real" was verified by making the whole reactor alkaline, which increases ascorbate reactivity and resulted in no detectable difference in O_2 signal with front guard on or off after 30 min (data not shown).

It is not a trivial task to calibrate a sensor in the range of 0-1 µmol L^{-1} as illustrated in Figs. 3 and 4. Even with a preincubation for 12 h of the initially N_2-bubbled water with ascorbate at neutral pH, we did not obtain an O_2 concentration of less than 100 nmol L^{-1} because of leakage of O_2 from the small Teflon-coated magnet in the flask. Only when the magnet was covered with glass was it possible to obtain the low initial O_2 concentration of 10 nmol L^{-1}.

The recording of a stable "zero signal" with the front guard on is usually obtained very quickly, with a typical 98% response of 5 s (Figs. 2 and 3). The oxygen signal for front guard cathode off is, on the other hand, often slowly drifting toward a stable value, and a 98% response time of 1-2 min at room temperature is typical. The sensor yielding the calibration data depicted in Figs. 3 and 4 exhibited an O_2 signal difference between vigorously stirred and stagnant water of 7% (data not shown). All data shown here are made with stirring—in situ mediated by currents and ship movements. The signal increased almost linearly (regression coefficients of 0.994-0.998) with increasing temperature in the range of 3°-30°C, and a slope of 0.0797 ± 0.0051 deg^{-1} (SD, $n = 3$) relative to the intercept of the regression line at 0°C. Thus, for in situ measurements, the signal U_T recorded at a given temperature T could be normalized to 0°C according to the trend line equation:

$$U_0 = U_T/(0.0797 \times T + 1). \quad (3)$$

Eq. 3 may be rewritten for normalization to a more relevant temperature as for example 10°C:

$$U_{10} = U_T/(0.0444 \times T + 0.556) \quad (4)$$

The observed temperature response is higher than previously reported for oxygen microsensors (Gundersen et al. 1998). The signal was further normalized to surface pressure in an analogous calculation assuming a relative, rather small change of –3% from 0 to 500 m (Glud et al. 2000). The long-term signal stability was checked for two newly constructed sensors over a period of 12 weeks of immersion in air-saturated water with continuous polarization. The variation in signal (normalized to an atmospheric pressure of 1050 hPa and 20°C) that was monitored every day during immer-

sion in constantly aerated water was within ± 2% of the signal on Day 1.

Measuring in the OMZ—Oxygen profiles were measured by the STOX sensor at 26 OMZ locations with a maximum deployment depth of 1000 m, but the results will be discussed elsewhere. Here we present data from a single rising CTD cast in Figs.5 to 8 to illustrate the performance of the STOX sensor during an in situ deployment. The O_2 distribution as obtained from the Seabird sensor (Fig. 5) exhibited a gradient from ~15 µmol L^{-1} at 450-500 m to less than 2 µmol L^{-1} at 330 m. From 330 to 115 m the profile was very smooth with a slight upward gradient. Small steps in the O_2 concentration at 120 and 200 m were associated with stops of the winch. At 115 m the signal rose abruptly and apparent O_2 concentrations varied between 2 and 3 µmol L^{-1} up to 45 m depth, above which an extremely steep gradient was located. Shown in Fig. 6 are the temperature and pressure compensated signals versus time for the STOX sensor (smoothed by taking a running 19-point average of the data points collected at a frequency of 25 s^{-1}), the output from a Seabird O_2 sensor, and the depth and temperature readings of the CTD. Shown in an insert are the raw data from the STOX sensor without temperature and pressure compensation. The timer in this first-generation in situ STOX electronics caused a noise signal when the front guard was turned on or off, and this generated the spikes (vertical lines) on the STOX signal seen in Fig. 6. There was a nice linear correlation between the temperature and pressure compensated STOX and Seabird O_2 signals (Fig. 7). The lowest data points for the Seabird sensor (white diamonds) were not included in the regression as they were affected by drift in signal for zero O_2 (see below).

For a correct interpretation of the results, it is most convenient to first have a closer look on the data from 201 to 31 m depth (i.e., from 2500 to 3700 second). At 201 and 120 m water depths, there was no visible difference between readings with the front guard on and off, indicating that these water masses were totally or almost anoxic. The Seabird sensor showed an apparent O_2 concentration drifting from 1.35 to 1.17 µmol L^{-1} while being in these anoxic water layers. At the subsequent stops at 100, 61, and 45 m depth, the Seabird sensor showed higher values of about 2.8, 3.0, and 2.1 µmol L^{-1} respectively, with no drift, which corresponds to 1.6, 1.8, and 0.9 µmol L^{-1} if we subtract the reading at 120 m, where oxygen was not detected by the STOX sensor.

A more accurate estimate of the O_2 concentrations within the OMZ core can be obtained with detailed comparison of the mean STOX sensor signal from 1 to 6 s (120 datapoints) before the front guard was turned on with the mean value 14 to 19 s after it was activated. For such an analysis, it is important to investigate each cycle individually, as any effect of drift in signal level thereby is minimized. The STOX sensor signal from the 5 complete cycles at rest at 201 m (3 cycles) and 120 m (2 cycles) water depths (Fig. 8) showed an average difference between front guard on/off of 0.000274 (± 0.000144, SD) V.

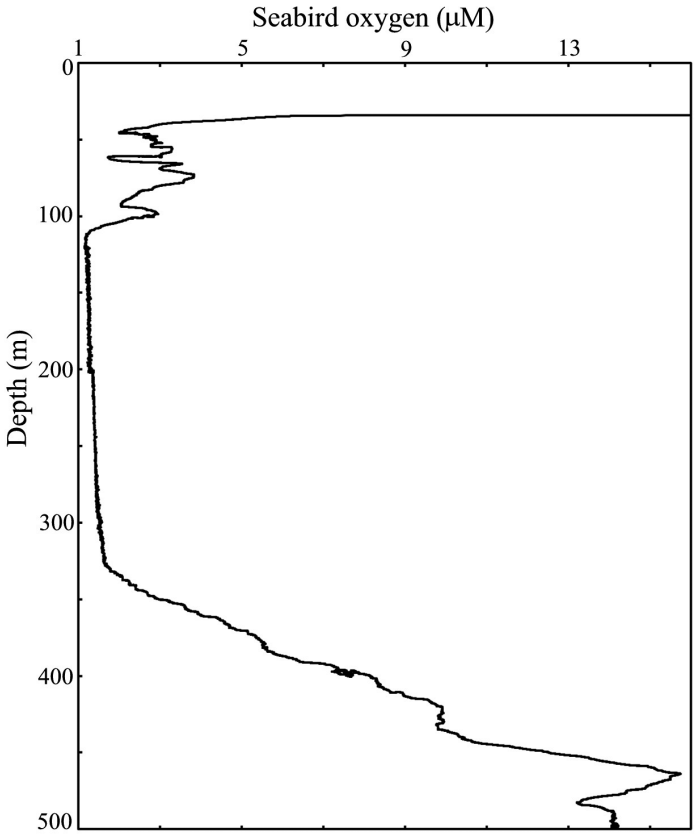

Fig. 5. Oxygen profile in the water masses off the Peruvian coast at depths varying from 500 m to 31 m as measured by the Seabird O_2 sensor during the upcast.

Converting to O_2 concentration using the slope of the STOX versus Seabird-O_2 regression (0.0936 V L µmol^{-1}; Fig. 7), we find that the water masses at 201 and 120 m water depth thus apparently contained 2.9 ± 1.5 nmol L^{-1} O_2. If the downward drift in STOX signal of 1.5 mV per 100 s during the measurement is taken into account, the estimate comes even closer to zero (0.3 ± 1.5 nmol L^{-1}) as the mean time difference between the on/off readings was 20 s, corresponding to a drift of 2.6 nmol L^{-1} O_2 during the determination. We thus obtain a result that within an accuracy of less than 2 nmol L^{-1} cannot be distinguished from absolute zero O_2.

We saw no indication of electronic offsets caused by the on-off front guard switching by the picoammeter channel used for the results presented here, but any small O_2 concentration measured by the STOX sensor should be interpreted as a maximum estimate as electronic offsets caused by for example humidity could interfere. We hold negative offsets, which would cause underestimation of O_2 concentrations, quite unlikely in our setup. If such an effect were indeed present, it is further unlikely that it should offset the measurements to result in values of 0.3 ± 1.5 nmol L^{-1} and never give negative readings, considering that the background current was about 20 pA (corresponding to 0.2 V meter output) and thus 2000 times higher than the cur-

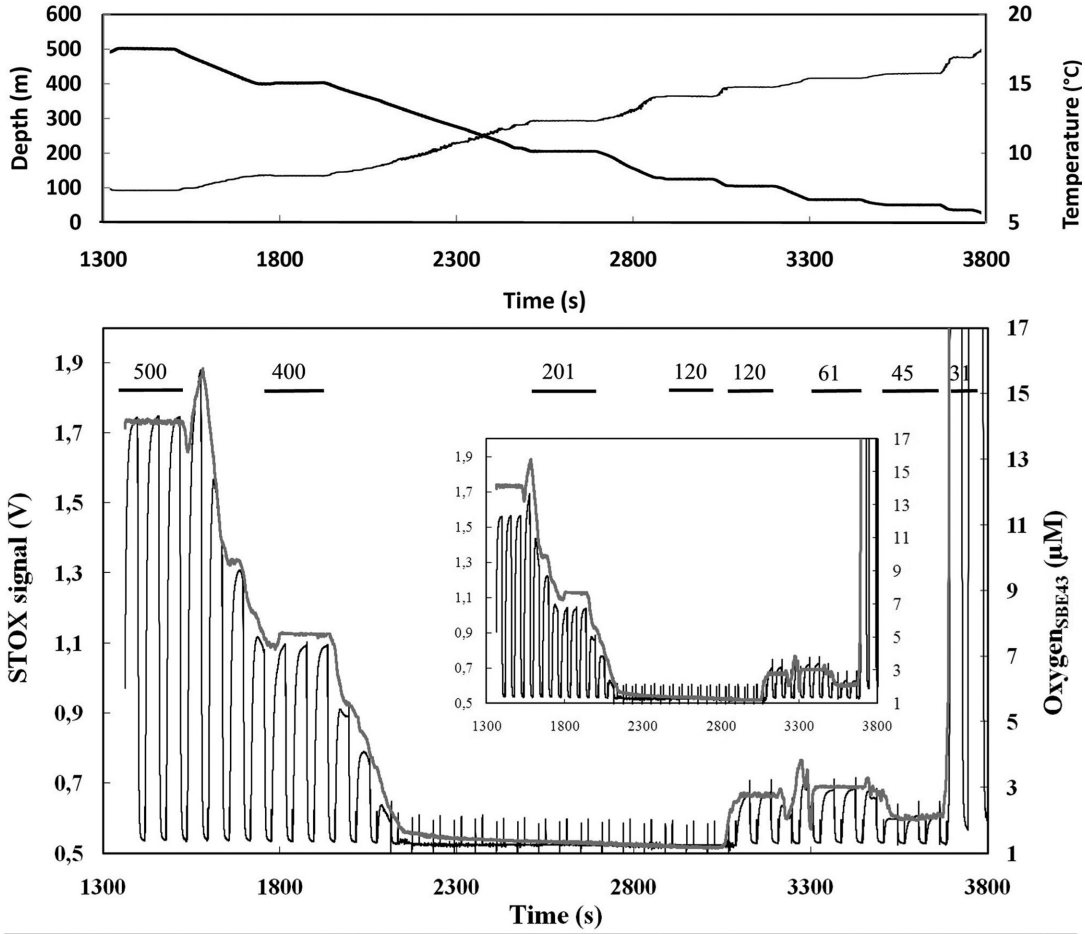

Fig. 6. Top panel: Temperature (thin line) and depth (thick line) as a function of time during the upcast deployment from which oxygen data are presented below. Lower panel: STOX microsensor (thin line with "spikes") and Seabird O_2 sensor (thick line) signals in the OMZ off the Peruvian coast at depths varying from 500 to 31 m. At 31 m the O_2 concentration increased to 92 µM and is thus off-scale on the present graphical representation. The spikes are an artifact caused by the timer-controlled on-off switching of the STOX sensor front guard. The baseline of 0.5 V corresponds to zero current in the sensor circuit. The water depths in meter are indicated at the top. Insert shows raw data from the STOX sensor without temperature and pressure compensation.

rent difference corresponding to 1 nmol L^{-1} O_2. For the investigated water-masses at 201 and 120 m depth, we can thus state that they contained < 2 nmol L^{-1} O_2. Similar results were obtained in several other casts (data not shown). We could have minimized the drift in STOX sensor signal by having the sensors turned on for several hours before the deployment and thereby have avoided the need to compensate for the (minimal) drift in signal. Also the data from the Seabird O_2 sensor would have exhibited considerably less drift if polarized for a several hours before deployment. However, due to the routine operation of the CTD unit at sea the sensors were only polarized about 1 h before deployment.

Reactor experiment—The data from the reactor experiment with OMZ water are shown in Fig. 9. Respiration caused a linear decrease in O_2 concentration from 120 to 0 nmol L^{-1} during the first 90 min of the incubation, corresponding to a respiration rate of 85 ± 3 nmol L^{-1} h^{-1}, and when the experiment was repeated at a slightly higher O_2 concentration the rate was estimated to be 93 ± 6 nmol L^{-1} h^{-1}. The subsequent addition of O_2 and 3 mL 7M $ZnCl_2$ to the reactor resulted in a stable O_2 concentration in the reactor of 556 ± 22 nmol L^{-1} over a 12-h period, verifying that the measured O_2 consumption rates were unaffected by O_2 leakage into the reactor.

The respiration rate of about 90 nmol L^{-1} h^{-1} is a very high rate and would make air-saturated water masses anoxic within 100 d. The water was taken in the upper part of the OMZ where respiration rates were supposed to be the highest, and irregular oxygen profiles in the upper OMZ, such as those shown in Figs. 5 and 6, indicate that eddies now and then may supply these water layers with new injections of oxygenated water. It should be noted that the rate of decrease was linear, indicating extremely low half-saturation (K_m) values for O_2 of the bacterial community. The measured values down to 20

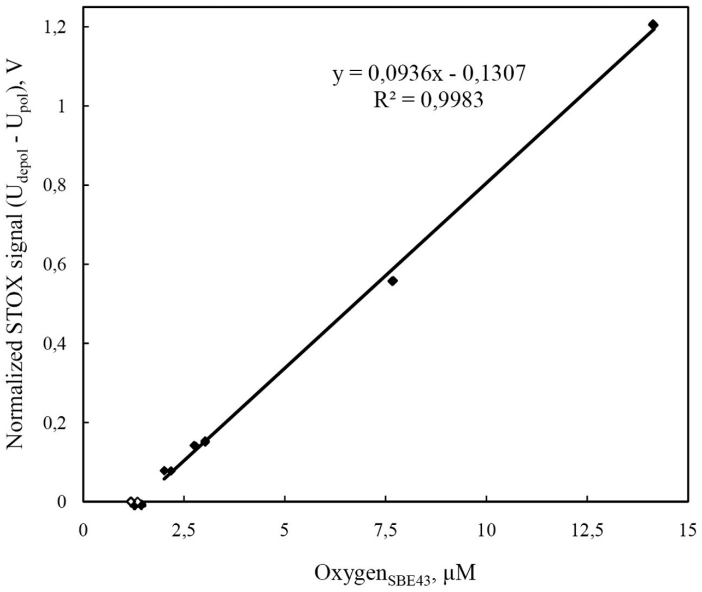

Fig. 7. STOX signal corrected for changes in temperature and pressure as a function of the Seabird O_2 reading from the same depths. The white diamonds representing zero signal from the STOX sensor were not included in the regression.

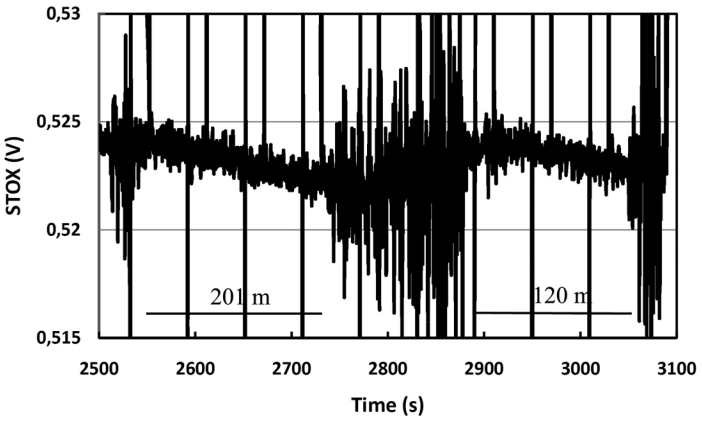

Fig. 8. The highly amplified STOX signal (total scale of 0.015 V corresponding to 1.5 pA or 160 nM O_2) for 201 and 120 m depth. The relatively high noise level from 2740 to 2890 s was caused by movement through the water column.

nmol L^{-1} indicate a linear decrease at least down to this concentration, so the community apparent K_m value must have been < 20 nmol L^{-1}. This result further emphasizes the need for highly sensitive techniques to study the effect of O_2 on microbial metabolisms. The reactor experiments were performed with manual operation of the front guard of the STOX sensor that was activated every 10-20 min. Continuous monitoring with an automatic timer operation of the sensor as performed with the all the other data shown in this article could have resulted in even more detailed data, but such equipment was not available on board the ship.

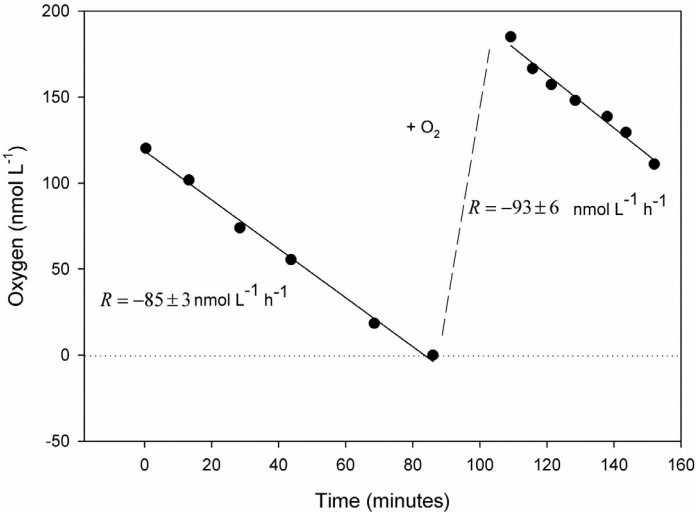

Fig. 9. Oxygen concentration as a function of time in a reactor containing a natural water sample from the oxygen minimum zone. Oxygen-saturated water was added twice. Oxygen decrease rates with standard deviations are indicated.

Discussion

Compared with normal oxygen sensors, the STOX sensor has its advantage in a very high degree of signal stability and thus reliability when measuring at very low O_2 concentrations. We are not aware of any other method that can be used to quantify O_2 concentrations in the range of 2–1000 nmol L^{-1} under difficult in situ conditions with large changes in temperature and hydrostatic pressure. We have not checked the signal stability of the sensor over periods of more than 12 weeks, where we observed excellent signal stability, and the sensor is actually not optimized for long-term signal stability yet. It is therefore recommended that for oceanographic measurements the sensor is used in combination with a standard amperometric or fluorescence-based oxygen sensor with better known stability characteristics, at least until more experience is obtained with long term stability under field use. In this study, we used the signal from the Seabird O_2 sensor for calibration of the STOX sensors, but with the current knowledge about the stability and temperature coefficients of the STOX sensors, it would be better to perform a direct calibration on deck before each deployment. One major obstacle against using a direct calibration in the present study was the limited resolution of the Seabird A/D converter, which made it necessary to sample only the signals for low oxygen concentrations. With a, for example, 16 bit A/D converter, it would be easy to use an air-equilibrated water sample for calibration during field use. For routine use of the STOX sensors at large depths, it will be necessary to analyze the pressure effect on several STOX sensors with a typical tip design. We are still making improvements on the design to optimize performance, but a pressure test should be performed when an optimal tip design has been approached.

It is evident from Figs. 6 and 7 that the Seabird O_2 sensor performed quite well, resolving changes of less than 1 µmol L^{-1}, but the zero value was drifting and was apparently deviating 1-2 µmol L^{-1} from the zero calibration performed before the Galathea3 expedition. Knowing from the STOX sensor data that the reading at 120 m depth represents < 2 nmol L^{-1} O_2, and that the change in SBE43 oxygen sensor signal between 200 and 120 m represents drift, we could use this reading as baseline instead, and we get very detailed data. The occurrence of a relatively thick water layer (> 50 m) with O_2 concentrations higher than 2 nmol L^{-1} and lower than 3 µM at the location described here (Figs. 5 and 6) was quite exceptional as compared with the situation at the upper OMZ boundaries at most of the other deployments, which showed very sharp transitions between anoxic water masses and waters with > 10 µmol L^{-1} O_2, but this profile very nicely illustrates the complete agreement between the values obtained with the STOX and the Seabird sensors.

For long-term deployment, biofouling is a problem with just about all types of measuring equipment, but the tiny tip of the STOX sensor offers less surface area for colonization. The rather low stirring sensitivity of the STOX sensor also reduces the impact of reduced water current in front of the sensor caused by fouling. Optodes are not affected by changes in water current due to fouling (Johnston and Williams 2006), but O_2 consumption within a biofilm covering the optode has the same impact on signal as by amperometric sensors.

With the STOX sensor, it is possible to resolve very low concentrations of O_2 without the need of frequent manual zero calibration, and this ability may be useful in many applications. It is, however, evident that the relatively long response time of the STOX sensors (i.e., the time for a full cycle) is a limiting factor for their application. For some applications, it is fully satisfactory to have data points spaced by, for example, 5 min. Yet, for use on a CTD, even the cycles of 1 min applied for our in situ experiments are too slow for routine analysis. The response time can be minimized by having thin membranes, a short distance between the membranes of inner and outer casing, and also by having the outer back guard very close to the tip of the inner oxygen sensor. In the present investigation, we have focused on having the highest possible current output and thus ability to detect very low concentrations. The sensors therefore had diameters of about 100 µm. Considerably faster responding sensors may be obtained by sensors with smaller diameter as the diffusion path thereby also can be made shorter, and a few sensors with internal tip diameters of about 50 µm and cycle times of down to 10 s at room temperature have been constructed. Due to the short diffusion paths, these sensors still had currents of 2-3000 pA for air saturation.

In situ analysis of the OMZ as performed here is an interesting application of the STOX sensor, and the proof of anoxia (i.e., < 2 nmol O_2 L^{-1}) in the central OMZ is an essential result. However, use of the STOX sensor in reactor experiments as also demonstrated here may be an even more interesting application. By use of this sensor, it is possible to perform experiments with seawater, bacterial cultures, etc. at low but controlled O_2 concentrations and thereby obtain detailed knowledge about kinetic parameters such as K_m values and thresholds for induction of various metabolic pathways.

Comments and recommendations

The main advantage by use of the STOX oxygen sensor is the ability to perform electronically induced zero point calibration during long-term deployment in natural waters, reactors, pipelines, etc., as this results in an extreme resolution of low oxygen concentrations. For normal oxygen monitoring tasks where oxygen concentrations are near air saturation other methods should be used, as they may be just as good as the STOX sensor to distinguish between say 200 and 201 µmol L^{-1}. The main disadvantage of the STOX sensor is the fragility. The thin tip may be shielded by a perforated tube and thereby be protected from mechanical damage, but mechanical shocks may cause cracks in the thin glass insulations inside the sensor or disrupt electrical connections. However, the shock sensitivity can no doubt be considerably reduced by gel filling and other modifications. Another disadvantage of the STOX sensor is a relatively high price from the commercial supplier (Unisense A/S) caused by the complex construction.

References

Bange, H. W., S. W. A. Naqvi, and L. A. Codispoti. 2005. The nitrogen cycle in the Arabian Sea. Prog. Oceanogr. 65:145-158.

Broenkow, W. W., and J. D. Cline. 1969. Colorimetric determination of dissolved oxygen at low concentrations. Limnol. Oceanogr. 14:450-454.

Devol, A. H. 1978. Bacterial oxygen-uptake kinetics as related to biological processes in oxygen deficient zones of oceans. Deep-Sea Res. 25:137-146.

Glazer, B. T., A. M. Marsh, K. Stierhoff, and G. W. Luther. 2004. The dynamic response of optical oxygen sensors and voltammetric electrodes to temporal changes in dissolved oxygen concentrations. Anal. Chim. Acta 518:93-100.

Glud, R., J. K. Gundersen, and N. B. Ramsing. 2000. Electrochemical and optical oxygen microsensors for in situ measurements, p. 195-222. *In* J. Buffle and G. Horvai [eds.], In situ monitoring of aquatic systems: Chemical analysis and speciation. Wiley.

Grasshoff, K. 1983. Determination of oxygen, p. 61-72. *In* K. Grasshoff, M. Ehrhardt, and K. Kremling [eds.], Methods of seawater analysis. Verlag Chemie GmbH.

Gundersen, J. K., N. B. Ramsing, and R. N. Glud. 1998. Predicting the signal of O_2 microsensors from physical dimensions, temperature, salinity, and O_2 concentration. Limnol. Oceanogr. 43:1932-1937.

Holmes R. M., A. Aminot, R. Kerouel, B. A. Hooker, and B. J. Peterson. 1999. A simple and precise method for measuring

ammonium in marine and freshwater ecosystems. Can. J. Fish. Aquat. Sci. 56:1801-1808.

Jensen, M. M., M. M. M. Kuypers, G. Lavik, and B. Thamdrup. 2008. Rates and regulation of anaerobic ammonium oxidation and denitrification in the Black Sea. Limnol. Oceanogr. 53:23-36.

Johnston, M. W., and J. S. Williams. 2006. Field comparison of optical and Clark Cell dissolved oxygen sensors in the Tualatin River, Oregon. Open-file report. http://pubs.usgs.gov/of/2006/1047/

Kuypers, M. M. M., and others. 2005. Massive nitrogen loss from the Benguela upwelling system through anaerobic ammonium oxidation Proc. Nat. Acad. Sci. 102:6478-6483.

Labasque, T., C. Chaumery, A. Aminot, and G. Kergoat. 2004. Spectrophotometric Winkler determination of dissolved oxygen: re-examination of critical factors and reliability. Mar. Chem. 88:53-60.

Luther III, G. W., and others. 2008. Use of voltammetric solid-state (micro)electrodes for studying biogeochemical processes: Laboratory measurements to real time measurements with an in situ electrochemical analyzer (ISEA). Mar. Chem. 108:221-235.

Martini, M., B. Butman, and M. J. Michelson. 2007. Long-term performance of the Aanderaa optodes and Sea-Bird SBE-43 dissolved-oxygen sensors bottom mounted at 32 m in Massachusetts Bay. J. Atmos. Oceanic Technol. 24:1924-1935.

Moffett, J. W., T. J. Goeffert, and S. W. A. Naqvi. 2007. Reduced iron associated with secondary nitrite maxima in the Arabian Sea. Deep-Sea Res. I 54:1341-1349.

Morrison, J. M., and others. 1999. The oxygen minimum zone in the Arabian Sea during 1995. Deep-Sea Res. II 46:1903-1931.

Patey, M. D., M. J. A. Rijkenberg, P. J. Statham, M. C. Stinchcombe, E. P. Achterberg, and M. Mowlem. 2008. Determination of nitrate and phosphate in seawater at nanomolar concentrations. Trends Anal. Chem. 27:169-182.

Paulmier, A., and D. Ruiz-Pino. In press. Oxygen Minimum Zones (OMZs) in the modern ocean. Progr. Oceanogr. Available online at www.science-direct.com from August 17, 2008.

Reimers, C. E., and R. N. Glud. 2000. In situ chemical sensor measurements at the sediment-water interface, p. 249-282. *In* M.S. Varney [ed.], Chemical sensors in oceanography. Gordon and Breach Science.

Revsbech, N. P. 1989. An oxygen microelectrode with a guard cathode. Limnol. Oceanogr. 34:472-476.

——— and B. B. Jørgensen. 1986. Microelectrodes: Their use in microbial ecology. Adv. Microb. Ecol. 9:293-352.

Thomas, R. C. 1978. Ion-sensitive intracellular microelectrodes. How to make and use them. Academic.

Submitted 16 October 2008
Revised 19 March 2009
Accepted 13 April 2009